

Accurate Formulas Locating Unstable Periodic Points in Chaos

Tetsushi Ueta and Kei Nagao

†Center for Advanced Information Technology, Tokushima University
 2-1, Minami-Josanjima, 770-8506 Japan
 Email: tetsushi@is.tokushima-u.ac.jp

Abstract—We have studied fractal nature of patterns given by the directional coloring for chaotic attractors. With this method, unstable periodic points are visualized as concentrated points or crossing points in the state space. A fractal pattern around the specific unstable fixed point are identified as a formula derived from relationship among neighbor unstable periodic points. In this paper, we try to model an accurate formula giving locations of unstable periodic points. Higher periodic points are predicted by the obtained formula. Some numerical examples are shown.

1. Introduction

Given two-dimensional discrete dynamical system, it is a burden toil to pick up unstable periodic points (abbr. UPPs) embedded in a chaotic attractor. We have studied fractal nature of patterns given by the directional coloring for chaotic attractors. With this method, UPPs are visualized as concentrated points or crossing points in the state space. A fractal pattern around the specific UPP are identified as a formula derived from relationship among neighbor UPPs. In this paper, we try to model an accurate formula giving locations of UPPs. Higher periodic points are predicted by the obtained formula. Some numerical examples are shown.

2. Invariant Patterns

Let us consider the following two-dimensional irreversible discrete system:

$$\mathbf{x}_{k+1} = \mathbf{f}(\mathbf{x}_k) \quad (1)$$

where, $\mathbf{x} = (x, y)$, and

$$\mathbf{f}(\mathbf{x}_k) = \begin{pmatrix} y_k + ax_k \\ x_k^2 + b \end{pmatrix}. \quad (2)$$

It exhibits a chaotic attractor at $a = 0.4$, $b = -1.24$, and theoretically many UPPs are embedded within it. Figure 1 show an 8-periodic and a 40 periodic orbits in the chaotic attractor. In general, locating UPPs are not so easy task for a given chaotic attractor and parameter values even if the system equation is explicitly obtained.

The directional coloring method[1] is a visualization scheme of chaos attractors that each mesh point in the state space is colored by the direction between the current point

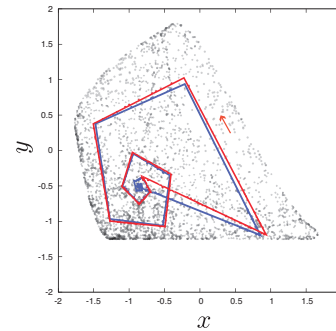


Figure 1: Unstable periodic points, $a = 0.4$, $b = -1.24$. Orange: 11 periodic, blue: 40 periodic orbits.

and its n -mapped point. Figure 2 shows the directional coloring result for Eq. (1) with $a = 0.4$, $b = -1.24$. Among (a) to (c), it is confirmed that a portion circled by a dashed line rotates and shrinks about the fixed point located in the center as n increases. In the past works[2][3], by using image processing technology, it is clarified that color concentrated or crossing points can be candidates UPPs. Figure 3(a) shows a magnified picture around the fixed point \mathbf{x}^* with evaluation of each 37-mapped points by directional coloring. The color-crossing points are specified by the arrows. points in which every color is terminated is specified by arrows, and they are candidates of UPPs. In fact, by using error collection method, accurate locations of UPPs are obtained from these candidates[1]. Notice that the point labeled by \mathbf{c}_{37} is the nearest 37-periodic unstable point for the fixed for \mathbf{x}^* . Figure 3 (b) and (c) show the locations of \mathbf{c}_{38} and \mathbf{c}_{39} for $n = 38$ and $n = 39$, respectively. As n increases, patterns are rotated, shrunk, and the new UPP \mathbf{c}_n is generated.

The rough location of \mathbf{c}_n is computed by an edge detection method[3], and a further error correction is done by Newton's method. We set an error tolerance for \mathbf{c}_n is less than 10^{-15} .

3. Fractal in patterns

Let us define $\epsilon_n = \|\mathbf{c}_n - \mathbf{x}^*\|_2$. This ϵ shrink exponentially as n increases. In Ref. [3], we derived a formula of the

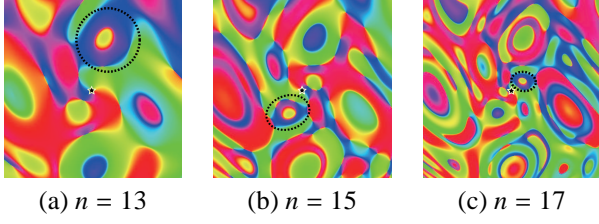


Figure 2: Patterns obtained by the directional coloring for Eq. (1).

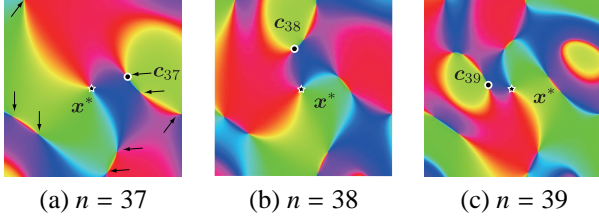


Figure 3: Pattern rotation and new c_n generation. Arrows indicate other candidate of UPPs.

absolute value of ϵ_n by sampling measurement:

$$\|\log_{10} \epsilon_n\|_2 \approx ax + b \quad (3)$$

where, a and b are constants, and they are depended on the parameter values. We compute them by the linear fitting with numerical solutions c_n . In the following, fitting parameters are obtained by the Marquardt-Levenberg algorithm (nonlinear least square estimation).

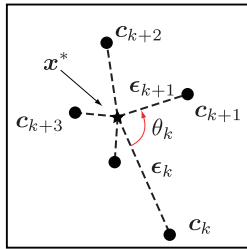


Figure 4: The definition of ϵ_k and θ_k .

In Fig. 5(a) shows actual value of $|\epsilon_n|$ and its fitted line. The red line is approximated as $\log_{10} \epsilon_n \approx -0.116n + 0.4$. A good agreement between them is confirmed.

Let us define θ_k as an angle determined by ϵ_{k+1} and ϵ_k . Plotted points in Fig. 5(b) indicate actual values of θ_n . The points alternatively jump up and down, thus it makes like a quasi periodic wave form (beat). We attach two sinusoidal curve to fit the envelope of the wave. The green and red lines are modeled as:

$$\theta_n = (-1)^n A \sin(\omega n + \phi) + b \quad (4)$$

where, $A = 0.303$, $\omega = 0.306$, $\phi = -0.588\pi$, $b = 1.42$. Over $n > 25$, plotted points and lines have a good agreement. From Eq. (4), the averaged angular is constant ($b \approx 0.45\pi$; the dashed line in Fig. 5(b)). These results specifies enough evidence of an existence of a logarithmic spiral, thus fractal nature is confirmed in the given chaotic attractor.

Many color-crossing points observed in Fig. 3 are simultaneously generated by increment of n . Since relative assignment of these points can be located from c_k in the invariant pattern, it is possible to locate and enumerate other UPPs by using an appropriate image processing.

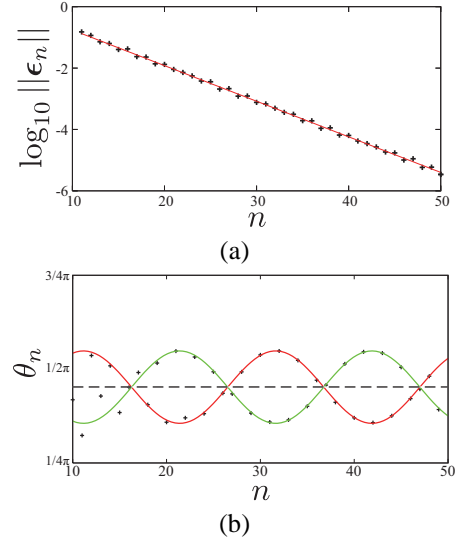


Figure 5: Distributions of the radius ϵ_n and angle θ_n by Eq.(3) and (4). Plotted points indicate numerical values of ϵ or θ_n .

4. Locating of UPPs

As an application of above approximation, in this paper, we try to derive a formula that locates the UPPs embedded in a chaotic attractor. Some modifications are applied for Eqs. (3) and (4) by using more precise fitting scheme, and we have the following equations:

$$\tilde{c}_n = \mathbf{x}^* + \sigma_n \begin{pmatrix} \cos S \theta_n \\ \sin S \theta_n \end{pmatrix}, \quad S \theta_n = \psi + \sum_{i=0}^{n-1} \theta_i. \quad (5)$$

where, ψ is the absolute angle between \mathbf{x}^* and c_0 . Then σ_n and θ_n are given as follows:

$$\begin{aligned} \sigma_n &= 10^{an+b+(-1)^n A \sin(\omega_1 n - \eta_1)} \\ \theta_n &= (-1)^n B \sin(\omega_2 n + \eta_2) + d, \end{aligned} \quad (6)$$

These functions can specify accurate locations of UPPs \tilde{c}_n by only substitution of n .

4.1. Example 1

Suppose we fix the parameter values for Eq. (1) as $a = 0.4$, $b = -1.24$, then we obtain the following parameters by using fitting method: $a = -0.1156$, $b = 0.4$, $A = 0.07$, $\omega_1 = 0.312$, $\eta_1 = 0.16\pi$ and $B = 0.31$, $\omega_2 = 0.306$, $\eta_2 = -0.572\pi$, $d = 1.418$. Figure 6 shows matching of \tilde{c}_k and c_k . The error between them is invisible.

It is noteworthy that the frequency components ω_1 and ω_2 are independent for the multiplier (eigenvalues) of the fixed point \mathbf{x}^* .

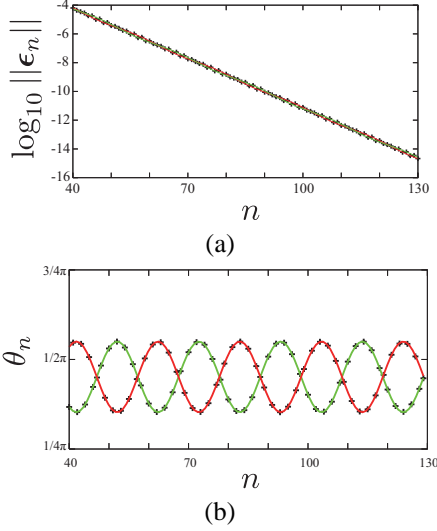


Figure 6: Relationship between n and ϵ_n for Example 1. Plotted points indicate numerical values of ϵ .

Both ϵ_k and θ_k are affected by sinusoidal functions of k , but they are not synchronized each other. We once tried an amplitude modulated wave for ϵ_k and θ_k models, but it failed. Two alternative (anti-phase) sinusoidal functions are essential.

Now we obtain an analytic formula that gives UPPs in the chaos attractor. If we want to know the location of c_k , the formula resulting the accurate location with specifying only k is very useful.

Figure 7 shows locations of UPPs. In this simulation, we use θ_{40} instead of ψ . Each vertex of the red line shows the location of c_k whose accuracy is guaranteed by Newton's method. While vertices on the black line are locations \tilde{c}_k . Please note that these lines do not show the part of the solution orbit like Fig. 1, but demonstrate a fractal nature of the chaotic attractor. In fact, a line in Fig. 7 forms a logarithmic spiral given by Eq.(6), i.e., ϵ_k and θ_k surely keep a certain scale. Note also that ψ in Eq. (5) is initialized by the value of c_{40} for this case.

4.2. Example 2

When we fix the parameters as $a = -0.1$, $b = -1.7$, a different invariant pattern of the directional coloring is shown

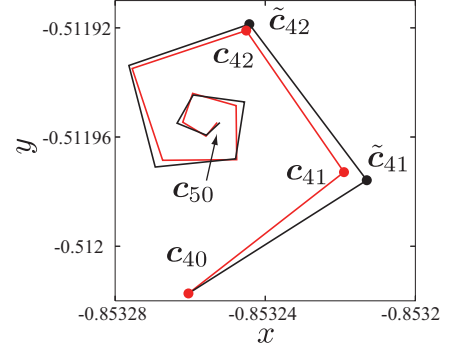


Figure 7: c_k (vertices of the red line) and \tilde{c}_k (vertices of the black line).

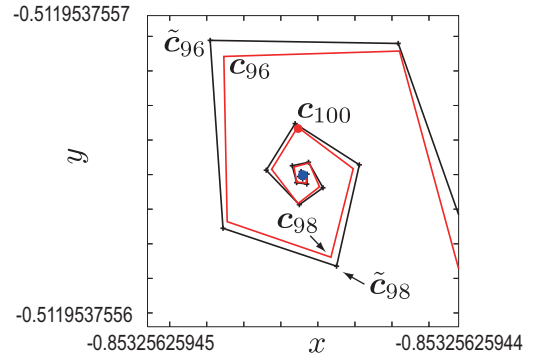


Figure 8: An enlargement of Fig. 7. c_k , $95 < k < 130$ are visualized.

in a chaotic attractor. Figure 9 depicts invariant patterns with $n = 34$ and $n = 35$ of the directional coloring around a UPP $\mathbf{x}^* = (-0.865097, -0.951606)$. The nearest radical point c_k is also an unstable k -periodic point.

For this example, Eq.(6) also acts reasonable. We have a very good fitting between \tilde{c}_n and c_n with this model. The fitting parameters are as follows: $a = -0.1185$, $b = 0.41$, $A = -0.07$, $\omega_1 = 0.08$, $\eta_1 = 0.477\pi$, $B = 0.27$, $\omega_2 = 0.08$, $\eta_2 = 0.0$, $d = 1.61$.

Figure 10 expresses agreement between \tilde{c}_k and c_k . The error between them is invisible. Figure 11 shows estimation errors defined as follows:

$$\begin{aligned} e_\epsilon &= \log_{10} \|\epsilon_n\| - \log_{10} \|\tilde{\epsilon}_n\| \\ e_\theta &= |\theta_n - \tilde{\theta}_n|. \end{aligned} \quad (7)$$

where, $\tilde{\epsilon}_n = \tilde{c}_n - \mathbf{x}^*$, and $\tilde{\theta}_n$ is an angle determined by \tilde{c}_n and \tilde{c}_{n+1} . Note that e_ϵ is on the logarithm scale, thus actual error between c_n and \tilde{c}_n becomes exponentially small as n increases. Actually -14 in logarithm scale approaches the limitation of a double precision register.

The mismatch between θ_n and $\tilde{\theta}_n$ can be evaluated good, that is, it is confirmed that the approximated analytic equation Eq. (6) describes the locations of UPPs. The error included in \tilde{c}_k comes seems to be modeling errors in Eq.

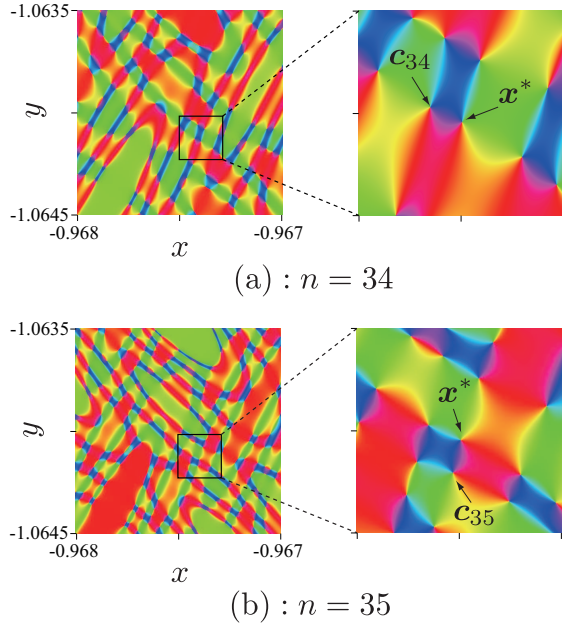


Figure 9: A directional coloring result for Eq. (1) with $a = -0.1, b = -1.7$. (a): $n = 34$, (b): $n = 35$.

(3), (4) and (5), however, the oscillation behavior in Fig11 implies existence of one or more frequency components. We should try to add more sinusoidal term in Eq.(6).

5. Conclusions

In this work, a fractal nature of a chaos in a two-dimensional discrete equation is shown. The analytic formula locating UPPs is derived and estimation errors are discussed. We only pay attention to the center 1-periodic UPP, this method also applicable for any UPP. Applying this method to other maps is a future problem.

References

- [1] T. Kumano, T. Ueta, H. Kawakami, "Pattern Emergence in Strange Attractor by Directions of Mappings," Proc. of ISCAS2006, pp.2737–2740, 2006.
- [2] K. Nagao and T. Ueta, "Detection of Periodic Points in 2D Nonlinear Maps by using Image Processing," Proc. IWVCC'08, pp. 110–113, Xi'an, China, Nov. 2008.
- [3] K. Nagao and T. Ueta, "A Structural Detection of Unstable Periodic Points in Chaotic Attractors by the Directional Coloring," Proc. NOLTA'09, pp. 419–422, Sapporo, Japan, Oct. 2009.

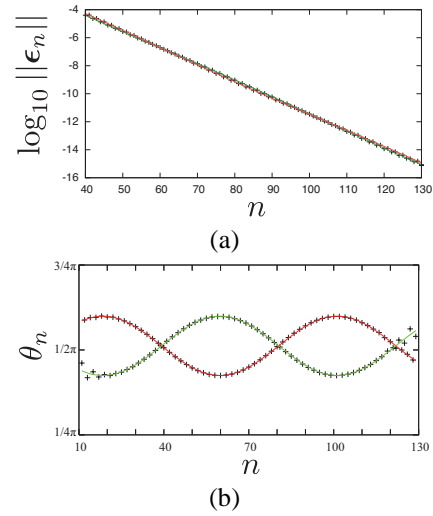


Figure 10: Relationship between n and ϵ_n for Example 2 for Example 2. Plotted points indicate numerical values of ϵ .

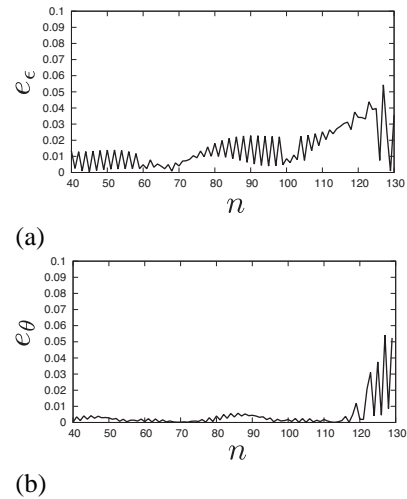


Figure 11: Estimation errors e_ϵ and e_θ .